

The non-convex shape of (234) Barbara, the first Barbarian ^{*}

P. Tanga,¹ B. Carry,² F. Colas,² M. Delbo,¹ A. Matter,^{1,3} J. Hanuš,^{1,4} V. Alí Lagoa,¹ A.H. Andrei,^{5,9,29} M. Assafin,⁵ M. Audejean,^{6,7} R. Behrend,^{6,8} J.I.B. Camargo,⁹ A. Carbognani,¹⁰ M. Cedrés Reyes,¹¹ M. Conjat,¹² N. Cornero,^{6,13} D. Coward,¹⁴ R. Crippa,^{6,15} E. de Ferra Fantin,^{11,16} M. Devogéle,¹⁷ G. Dubos,¹³ E. Frappa,¹⁸ M. Gillon,¹⁷ H. Hamanowa,^{6,19} E. Jehin,¹⁷ A. Klotz,²⁰ A. Kryszczyńska,²¹ J. Lecacheux,²² A. Leroy,^{6,23} J. Manfroid,¹⁷ F. Manzini,^{6,24} L. Maquet,² E. Morelle,^{6,25} S. Mottola,²⁶ M. Polińska,²¹ R. Roy,^{6,27} M. Todd,¹⁴ F. Vachier,² C. Vera Hernández,¹¹ P. Wiggins²⁸

¹Laboratoire Lagrange, UMR7293 CNRS, UNS, Observatoire de la Côte d’Azur, Nice, France

²IMCCE, Observatoire de Paris, UMR8028 CNRS, France ³Max Planck Institut für Radioastronomie, Bonn, Germany ⁴Astronomical Institute, Faculty of Mathematics and Physics, Charles University in Prague, Czech Republic ⁵Observatório do Valongo/UFRJ, Brazil

⁶CdR & CdL Group: Lightcurves of Minor Planets and Variable Stars, Switzerland ⁷Observatoire de Chinon, Chinon, France

⁸Geneva Observatory, Switzerland ⁹Observatório Nacional/MCTI, Brazil ¹⁰Osservatorio Astronomico della regione autonoma Valle d’Aosta, Italy

¹¹Agrupación Astronómica de Fuerteventura, Spain ¹²Observatoire de Cabris, France ¹³Association des Utilisateurs de Détecteurs Électroniques (AUDE), France ¹⁴Department of Imaging and Applied Physics, Curtin University of Technology, Bentley, Australia

¹⁵Osservatorio astronomico di Tradate, Italy ¹⁶Academia de ciencias e ingenierias de Lanzarote, Arrecife, Spain ¹⁷Institut d’Astrophysique, Géophysique et Océanographie, Université de Liège, Belgium

¹⁸Euraster, St. Etienne, France ¹⁹Hamanowa Astronomical Observatory, Fukushima, Japan

²⁰CNRS, IRAP, Toulouse, France ²¹Astronomical Observatory Inst., Faculty of Physics, Adam Mickiewicz University, Poznań, Poland

²²LESIA-Observatoire de Paris, CNRS, UPMC Univ. Paris 06, Univ. Paris-Diderot, Meudon, France ²³Association T60, Toulouse, France

²⁴Stazione Astronomica di Sozago, Italy ²⁵Lauwin Planque, France ²⁶Institute of Planetary Research, German Aerospace Center, Berlin, Germany

²⁷Blauvac Observatory, St.-Estève, France ²⁸Wiggins Observatory, Tooele, UT, USA ²⁹SYRTE, Observatoire de Paris, France

3 February 2015

ABSTRACT

Asteroid (234) Barbara is the prototype of a category of asteroids that has been shown to be extremely rich in refractory inclusions, the oldest material ever found in the Solar System. It exhibits several peculiar features, most notably its polarimetric behavior. In recent years other objects sharing the same property (collectively known as “Barbarians”) have been discovered. Interferometric observations in the mid-infrared with the ESO VLTI suggested that (234) Barbara might have a bi-lobated shape or even a large companion satellite. We use a large set of 57 optical lightcurves acquired between 1979 and 2014, together with the timings of two stellar occultations in 2009, to determine the rotation period, spin-vector coordinates, and 3-D shape of (234) Barbara, using two different shape reconstruction algorithms. By using the lightcurves combined to the results obtained from stellar occultations, we are able to show that the shape of (234) Barbara exhibits large concave areas. Possible links of the shape to the polarimetric properties and the object evolution are discussed. We also show that VLTI data can be modeled without the presence of a satellite.

Key words: asteroid – shapes – occultations – photometry – interferometry

1 INTRODUCTION

The physical characterization of asteroids is of primary importance for understanding their origin and evolution. Sim-

ple information such as rotation period and direction of the spin axis have been related to evolutionary processes such as accretion in the protoplanetary disk (Johansen & Lacerda 2010), impacts (Takeda & Ohtsuki 2007b, 2009b; Marzari et al. 2011; Holsapple & Housen 2012), thermal forces (Bottke et al. 2006), internal cohesion and degree of fragmentation (Holsapple 2007), to cite a few notable examples.

Asteroid (234) Barbara exhibits peculiar features, such

^{*} Based in part on observations collected at the European Organization for Astronomical Research in the Southern Hemisphere, Chile - program ID: 076.C-0798.

as an anomalous polarimetric behavior (Cellino et al. 2006), a possible very irregular shape, a suspected large companion (Delbo et al. 2009), a long rotation period (Schober 1981), as detailed in Sect. 2. Polarimetry and near-infrared spectroscopy suggest that (234) Barbara and other similar asteroids could be composed by high fraction of the most ancient solids formed in the Solar System, the Ca-Al-rich Inclusions (CAI, see Sunshine et al. 2008).

These properties motivated a focused study of this target, given the substantial lack of other physical data. Here we address in particular the determination of the shape and the infirmation of the binary hypothesis. We proceeded by setting up a long and intense campaign of photometric observations, complemented with two stellar occultations.

Traditional lightcurve inversion (e.g., Kaasalainen & Torppa 2001; Kaasalainen et al. 2001), retrieving complex shapes described by several parameters, converge to a unique solution only under the hypothesis of convexity of the shape. In the specific case of (234) Barbara, an imposed convexity could hide the evidence of a bi-lobated structure, responsible of the suspected presence of a satellite (Delbo et al. 2009).

Given the limitations of photometry when taken alone, we also apply the inversion algorithm KOALA (Carry et al. 2010; Kaasalainen 2011), which can use data coming from different sources for deriving a consistent, unique model of an asteroid. Its main applications have concerned the joint inversion of photometry, disk-resolved imaging and stellar occultations. We illustrate in the following the results that we obtained on the asteroid (234) Barbara by this approach.

Our efforts were focused on an observation campaign in the period 2008-2011 (plus some additional data in 2014), involving both time-series photometry and stellar occultations, whose results are presented in Sect. 3.1 and 3.2. We were able to invert both photometric and occultation data for deriving a 3-D shape model, as described in Sect. 4. We use this model to validate the interferometric observations at VLTI presented by Delbo et al. (2009), and eventually discuss the implications of our results.

2 PECULIARITIES OF (234) BARBARA

Barbara is an asteroid belonging to the inner Main Belt, classified for a long time as a S type (Tedesco 1989). Its slow rotation (about 26.5 hours) was discovered by Schober (1981). A detailed, dedicated, physical characterization for this object was not attempted in the past, with the exception of spectroscopy. Owing to a slight excess in reflectance in the red part of the spectrum with respect to the core of the S class, followed by a flat plateau in the near-infrared, Barbara was classified Ld in the Bus & Binzel (2002) taxonomy. From thermal radiometry with IRAS, a diameter of 44 ± 1 km was derived (Tedesco et al. 2002) corresponding to a geometric albedo $p_v = 0.22 \pm 0.01$ (assuming an absolute magnitude of $H = 9.02$). Other available size determinations involve AKARI (47.8 ± 0.68 km) and the Wide Infrared Survey Explorer (WISE). WISE yielded two measurements, but one of them is clearly discrepant. We discuss this issue in detail and provide a new, coherent diameter determination, in Sect. 4.

Cellino et al. (2006) pointed out that this asteroid has an unusual polarimetric behavior. The degree of linear po-

larization of sunlight scattered by asteroid surfaces exhibits a variation as a function of the illumination conditions, described by means of the phase angle, namely the angle between the directions to the Sun and to the observer, as seen from the asteroid. In particular, the morphology of the phase-polarization curve has some general properties which, apart from some differences related mainly to the geometric albedo of the surface, tend to be shared by all known asteroids. The case of (234) Barbara is different, as it exhibits a “negative polarization branch” wider than usual, with an “inversion angle” around 30° , a much larger value with respect to the $\sim 20^\circ$ displayed by other objects (for details see Cellino et al. 2006). We recall here that the negative polarization corresponds to a polarization plane parallel to the scattering plane.

A very similar phase-polarization curve was found later on for other L, Ld and K-type asteroids (Gil-Hutton et al. 2008; Masiero & Cellino 2009), collectively known as “Barbarians” from the first discovered. Data concerning the asteroid (21) Lutetia seems to indicate also a peculiar polarization, but with a lower inversion angle (Belskaya et al. 2010) intermediate between *regular* asteroids and *Barbarians*.

Several hypothesis have been formulated in the past for explaining the high fraction of negative polarization. In particular, the role of coherent backscattering (Muinonen et al. 1989; Shkuratov et al. 1994) was invoked, normally associated to high albedos producing narrow and strong opposition peaks in the phase-brightness curve. Another possibility is single particle scattering (Muñoz et al. 2000; Shkuratov et al. 2002) on refractory inclusions. In fact, among meteorites, some carbonaceous chondrites (type CV3 and CO3) produce the highest negative polarization, which could be related to the abundance of fine-grained Ca-Al refractory inclusions (CAI) (Zellner et al. 1977). Burbine et al. (1992) suggested that (980) Anacostia, another object having polarimetric properties similar to (234) Barbara, could be a spinel-rich body with a mineralogy similar to CO3/CV3 meteorites. The reason of the negative polarization should then be related to the fine-grained structures of white spinel inclusions surrounded by a dark matrix (Burbine et al. 1992). Sunshine et al. (2008) reached similar conclusions for Barbara itself by comparing its visible and IR spectra to laboratory spectra of CAI materials. Surprisingly, a satisfactory match can be reached only when the fraction of spinel-bearing CAIs is very high (up to 30% for explaining the spectral features observed). If this finding were true, the Barbarians should have formed in a nebula rich of refractory materials, and would be among the most ancient asteroids formed. No sample with high percentages of CAI is present in the current meteorite collections.

If mineralogy is the culprit for the polarization anomaly, it is then not surprising that all Barbarians belong to a similar spectral class. At first sight, it is unclear why not all other L, Ld, and K asteroids (and more in general the whole S-complex) do not share similar polarization properties. For example the L-type (12) Victoria has a usual polarization with inversion angle $\sim 20^\circ$. However, if the near-IR spectrum is considered, all Barbarians belong to the same L class as defined by (De Meo et al. 2009).

Cellino et al. (2006) suggested that anomalous polarization could be due to large-scale concavities responsible of introducing a distribution of scattering and incidence an-

gles different from those of a regular, convex surface. This conjecture has never been proven to play a role, essentially due to the lack of measurements at high phase angles of objects known to have large concave features. Also, theoretical models do not seem to explore explicitly this possibility.

Asteroid (234) Barbara was one of the targets chosen for the first interferometric observations of asteroids by the Very Large Telescope Interferometer (VLTI), using the MID-infrared Interferometer (MIDI, [Leinert et al. 2003](#)). This instrument can reach an angular resolution in the range 20-200 mas, depending on the choice of the baseline. It can thus be used to measure the apparent size of asteroids, by modeling the visibility of the interferometric fringes, independently from other common methods, such as thermal infrared radiometry. It can also be used to detect and study the orbit of multiple asteroid systems. VLTI-MIDI observations, obtained in November 2005, yielded an average diameter of 44.6 ± 0.3 km. These observations and their processing are extensively described in [Delbo et al. \(2009\)](#). Their main result, obtained by modeling the VLTI visibility function, is the detection of a signature of duplicity of the source. In fact, they show that a fit with a single object cannot reproduce the data. A satisfactory fit requires a second component. The resulting system, composed by two uniform disks ~ 37 and ~ 21 km in diameter, could be interpreted either as a single object of irregular shape, or as a binary close to the alignment with the line of sight. This model is reproduced for ease of comparison in Fig. 6.

The unambiguous hints of a binary or bi-lobated body has been an additional motivation for our focused study of (234) Barbara. We stress here that we don't use VLTI data in the shape determination process described below (a rather difficult task to the very different nature of such data). Conversely, we will test our derived shape against the VLTI observations.

Very recently, by observing the polarization properties of the members of the high-inclination dynamical family of the L-type (729) Watsonia, [Cellino et al. \(2014\)](#) discovered that it is composed by Barbarians. This fact seems to indicate that the Barbarian character is intrinsic to bulk properties of the body, not only to some surface effects. In fact, if the anomalous polarization was limited to a surface process, the parent body shattering and the subsequent fragment mixing, would strongly dilute the polarimetric signature of the original surface on the family members.

3 OBSERVATIONS

3.1 Photometric campaign

We obtained R-band photometry of Barbara starting in June 2008. The most recent observations that we use in our data reduction have been acquired in February 2014. Given the long rotation period, a single site is highly inefficient in covering a full rotation. We thus put at contribution many observers and telescopes, at widely different longitudes. Thanks to this considerable, shared effort we were able to provide an adequate coverage of the brightness variations.

In Table 1 we list the different photometric data sets that we used for this study. A sample lightcurve is presented in Fig. 1. This result is the composite of 13 observing

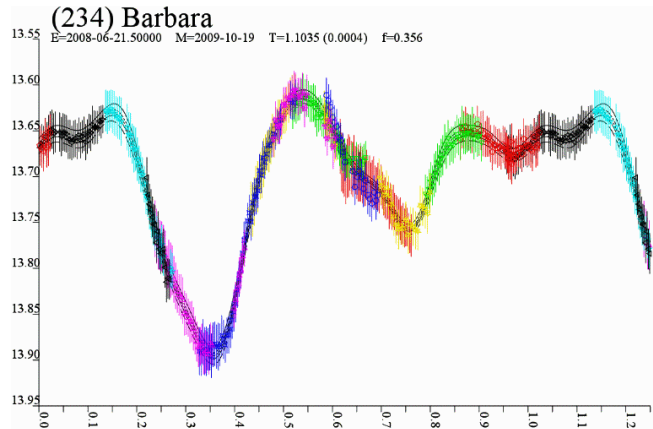


Figure 1. Lightcurve obtained in June 2008 over 13 days by M. Conjat (from the main OCA site) and P. Tanga (Tourrette-Levens, private facility), folded on the rotation period of 26.474 h. Each color represents a different observing session. As the observing sites were in the same geographic area, several nights were needed to cover the entire rotation. The curve qualitatively represents the amplitude and shape of the brightness variation, hinting to an irregular body.

sessions spanning ~ 6 weeks, from two sites very close in longitude. Over this time, the object changes its geometry, relative to the Sun and to the observer, thus introducing potentially complex variations that are not linked to the object rotation alone. In particular, phase angle variations can rapidly change shadowing effects. For this reason the folded lightcurve has just an indicative value. From a qualitative point of view, it is however interesting to note that the amplitude is rather large and the variation complex.

We can judge the long-term photometric coverage by considering the ranges of ecliptic heliocentric longitudes corresponding to the three apparitions over which the asteroid was observed. We thus obtain $\sim 357^\circ$ in September 1997, 260° in June 2008, 160° - 180° in the period November 2010 - April 2011, and 120° in February 2014. The distribution over different values in ecliptic longitude favors the coverage of the largest possible range of aspects angle allowed by the pole obliquity.

3.2 Stellar occultations

Two stellar occultations by (234) Barbara were successfully observed by our team and collaborators, on October 5, 2009 and only a few weeks later, on November 21, 2009. Both target stars had a magnitude $V < 8$, which greatly facilitated the use of portable instruments and the deployment of several stations.

The first event took place on the Atlantic Ocean, with a predicted path passing on Canary Islands and central Africa. An expedition from France installed portable observing stations on the islands of Fuerteventura and Lanzarote (southern tip). Local amateur astronomers contributed with equipment at further sites, and logistic support. Good weather granted nearly optimal conditions and several chords of the occultation were recorded (see Table 2). The positive result showed that the prediction was very accurate, the real

Table 1. Photometric observing runs used to derive the shape of (234) Barbara. The full table is available among the online resources. Legend: \aleph : 0.32 m Observatoire du Chinon (France): M. Audejean. b : 0.40 m, Hamanowa Astronomical Observatory (Japan): H. & H. Hamanowa. \square : 0.4 m Observatoire de la Côte d’Azur (France): M. Conjat; and 0.2 m Specola Tourrette Levens: P. Tanga. \uplus : From Schober (1981).

Session start (yyyy-mm-dd hh:mm)				Duration (min.)	N obs.	Notes
1979	09	13	05:11	262	138	\uplus
1979	09	14	01:54	455	212	\uplus
1979	09	15	02:06	437	64	\uplus
2008	06	18	20:56	226	51	\square
2008	06	19	20:46	236	41	\square
2008	06	20	20:58	279	34	\square
2008	06	21	20:41	313	52	\square
2008	06	22	20:45	291	41	\square
2008	06	23	20:35	216	34	\square
2008	06	25	20:41	283	50	\square
2008	06	26	20:45	256	46	\square
2008	06	27	21:21	182	41	\square
2008	06	28	21:18	157	36	\square
2009	11	18	23:21	22	51	\aleph
2009	11	24	23:16	121	25	\aleph
2009	11	25	22:55	160	13	\aleph
2009	11	25	12:41	206	17	b

...
Complete table available in the online resources.

shadow being shifted southward relatively to predictions by ~ 10 km only.

The high reliability of the asteroid positional ephemeris was a precious information for planning the deployment of the observers around the path of the following event. Several astronomers in the United States gathered in Florida and few others in central Europe at the oriental extreme of the path. The noticeable effort for the deployment of several automated stations by single observers was successful, thus securing a dense set of occultation chords (Table 3). For both events the entire data set is available, for example, at PDS¹ (Dunham et al. 2011).

Data reduction of the occultation on October 5, 2009 event results in the strong hint of an elongated, oval shape (Fig. 2), with possible irregular features. The observed chords on November 21, 2009 consistently draw an overall triangular shape, with a large and pronounced concavity at the South limb, and hints of other minor concavities (Fig. 2). Both occultations provide an average size consistent with the results obtained at VLTI (Sect. 4).

Other occultation events by Barbara were observed later on. We neglect here the results obtained on December 14, 2009 in the USA, given that only 3 chords are available (Dunham et al. 2011). Also, positive observations of the occultation on January 17, 2010, obtained in Japan, have not been used as the faintness of the target star ($V=12.0$) prevented accurate timings.

None of the observed occultations presents secondary events linked to the presence of possible satellites in proximity of the primary body.

4 SHAPE AND SPIN DETERMINATION OF (234) BARBARA

As the occultations indicate the clear presence of concavities and the lightcurve is rather irregular, a simultaneous inversion by KOALA of photometry and occultation data

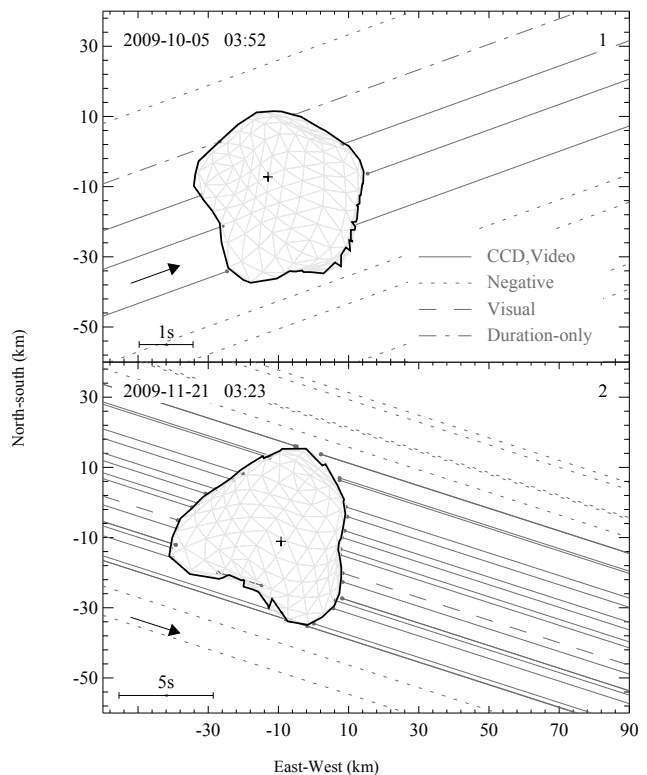


Figure 2. Plot on the plane of the sky of the occultation chords reported in Tables 2 and 3. The different line formats distinguish among positive observations (CCD, Video), negative ones, visual timings, and duration measurements. The profile of (234) Barbara at the epoch of each occultation, as derived by the shape model presented in this article, is represented by the black contours.

appeared necessary (see Kaasalainen 2011; Carry et al. 2010, 2012, for a description of the algorithm). For a further consistency check we also ran the usual lightcurve-only inversion (e.g., Kaasalainen & Torppa 2001; Kaasalainen et al. 2001)

¹ <http://sbn.psi.edu/pds/resource/occ.html>

Table 2. Observers and chords for the occultation of HIP32822 ($V=7.77$), on 2009 October 5. The UT columns contain the epochs associated to each chord. In the “Event” column, the flags can be: M = missed, no occultation observed; D = disappearance; and R = reappearance. Uncertainties on timing in seconds at the $3\text{-}\sigma$ level are provided. Some observers were capable of deploying multiple stations, so their name appear more than once.

#	Observer and site	UT	Event	3σ	UT	Event	3σ
1	Vachier, Morro del Jable, Spain		M			M	
2	Vachier, Costa Calma, Spain		M			M	
3	Lecacheux, Gran Tarajal, Spain		M			M	
4	Maquet, Tuineje, Spain		M			M	
5	Lecacheux, Antigua, Spain	04 10 22.02	D	0.03	04 10 24.50	R	0.03
6	Maquet/de Ferra/Cedr�s, Tefia, Spain	04 10 22.25	D	0.02	04 10 25.11	R	0.02
7	Colas/Vera, La Oliva, Spain	04 10 22.44	D	0.02	04 10 25.21	R	0.02
8	Colas, Corralejo, Spain	04 10 23.50	D	0.15	04 10 24.96	R	0.15
9	Tanga, Playa Blanca, Spain		M			M	

Table 3. Similar as Table 2, for the occultation of the star HIP34106 ($V=7.5$), on 2009 November 21.

#	Observer and site	UT	Event	3σ	UT	Event	3σ
1	Harris, Deltona, FL, USA		M			M	
2	Dunham, Okahumpka, FL, USA		M			M	
3	Dunham, Center Hill, FL, USA		M			M	
4	Venable, Webster, FL, USA		M			M	
5	Venable, Tarrytown, FL, USA		M			M	
6	Venable, Tarrytown, FL, USA	03 38 34.27	D	0.03	03 38 35.62	R	0.03
7	Dunham, Groveland, FL, USA	03 38 32.77	D	0.10	03 38 34.21	R	0.10
8	Maley, Clermont, FL, USA	03 38 32.18	D	0.05	03 38 36.01	R	0.05
9	Fernandez/N Lust, Orlando, FL, USA	03 38 26.70	D	0.50	03 38 30.60	R	0.50
10	Dunham, Green Pond, FL, USA	03 38 32.63	D	0.02	03 38 38.37	R	0.02
11	Maley, Polk City, FL, USA	03 38 32.82	D	0.02	03 38 39.16	R	0.02
12	Turcani, Christmas, FL, USA	03 38 27.30	D	0.10	03 38 34.50	R	0.10
13	Bredner, Germany	03 18 12.40	D	–	03 18 18.70	R	–
14	Maley, Polk City, FL, USA	03 38 33.90	D	0.10	03 38 41.50	R	0.02
15	Maley, Polk City, FL, USA	03 38 34.52	D	0.02	03 38 42.79	R	0.02
16	Povenmire, Deer Park, FL, USA	03 38 28.30	D	0.30	03 38 37.50	R	0.30
17	Denzau, Panker, Germany	03 18 02.68	D	–	03 18 10.64	R	–
18	Maley, Polk City, FL, USA	03 38 34.61	D	0.02	03 38 43.85	R	0.02
19	Iverson, Harmony, FL, USA	03 38 30.95	D	0.02	03 38 40.23	R	0.02
20	Coles, Harmony, FL, USA	03 38 30.73	D	0.03	03 38 40.01	R	0.03
21	Degenhardt, Deer Park, FL, USA	03 38 29.61	D	0.02	03 38 38.77	R	0.02
22	Degenhardt, Deer Park, FL, USA	03 38 36.26	D	0.02	03 38 38.79	R	0.02
23	Degenhardt, Deer Park, FL, USA	03 38 29.96	D	0.02	03 38 33.96	R	0.02
24	Degenhardt, Deer Park, FL, USA	03 38 31.70	D	0.10	03 38 33.50	R	0.02
25	Degenhardt, Deer Park, FL, USA	03 38 32.23	D	0.02	03 38 33.16	R	0.02
26	Degenhardt, Deer Park, FL, USA	03 38 33.27	D	0.02	03 38 33.40	R	0.02
27	Degenhardt, Deer Park, FL, USA		M			M	
28	Bulder, Buinerveen, The Netherlands		M			M	

to retrieve a convex model, the close envelope of the concave shape.

In running the pure photometric inversion, we decided to include sparse photometry to better constrain rotation period and spin vector coordinates, to compensate the short coverage of lightcurves induced by the long rotation period of Barbara. The whole procedure is described in detail in (Hanus et al. 2013). In our case we selected 182 and 124 photometric measurements coming from the USNO–Flagstaff station (IAU code 689) and the Catalina Sky Survey (IAU code 703, ?), respectively, that were added to our collection of 57 dense lightcurves. We started by searching for optimum sidereal rotation period, by using the `period.scan` software, available on DAMIT² (Durech et al. 2010), on the combined data set of lightcurves and sparse photometry (Fig. 3). Starting from the best-fit period of 26.4744 h, we then explored the possible locations of the spin-vector coordinates. We ran a full exploration of the ecliptic J2000 celestial sphere (λ, β)

Table 4. Shape and spin vectors for (234) Barbara. In the bottom section, the overall shape parameters (axis ratios of the best-fitting ellipsoid) are listed.

Parameter	light-curve only	KOALA	Unit
Period	24.4744 ± 0.0001	24.4744 ± 0.0001	h
Pole (λ, β)	(156, -46)	(144, -38)	deg.
D_V		46.3 ± 5	km
a/b	1.12	1.11	
b/c	1.59	1.14	

by keeping the period fixed. For each position of the spin axis we computed the residuals of the model-derived brightness, with respect to the photometric measurements. The resulting map of residuals is shown in Fig. 4. The resulting pole coordinates and rotation periods are in Table 4.

At negative latitudes, several minima in the residual map appear. The two deepest ones (around $\lambda \sim 150^\circ$ and 290°) are both candidates for the spin axis direction. The fact that the solution is not unique clearly illustrates the

² <http://astro.troja.mff.cuni.cz/projects/asteroids3D/>

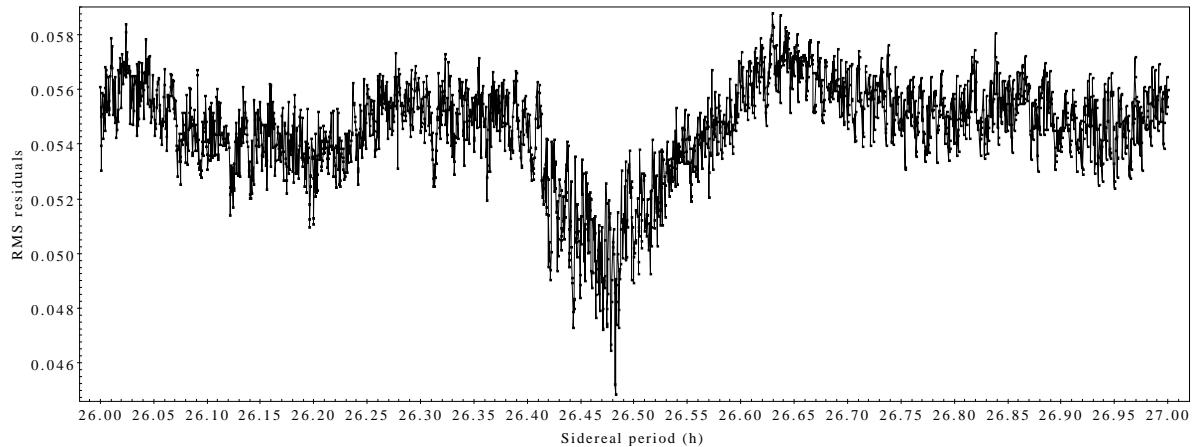


Figure 3. The RMS deviation of the photometry relative to the convex model, against sidereal rotation period.

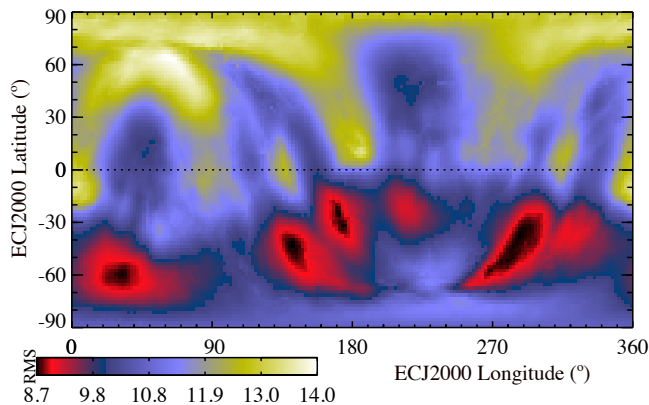


Figure 4. The RMS deviation of the photometry relative to the convex model, obtained by exploring the whole space of pole coordinates. In the plot, the ecliptic longitude λ is on the horizontal axis, and the ecliptic latitude β on the vertical. Red and black values visualize the position of the minima.

challenge of the inversion process, despite the large number of lightcurves available. This is most probably due to the rather slow rotation. In such conditions, all the lightcurves embrace only very limited portion of the entire rotation (less than 20% on average).

As the convex solution is not perfectly constrained, the computation of a shape without the convexity constraint (i.e., with concavities) might appear as an academic exercise. However, the concavities explored by the occultations are well constrained by the accuracy and the consistency of the timings, in particular for the event of November 21, 2009. For this reason, it seemed appropriate to attempt an inversion by KOALA, including both occultations and photometry. In the process, KOALA adapts the concavities to the occultations, but will also tend to create other less-constrained concavities to better reproduce the photometry. For this reason the result should not be taken at face value. Nevertheless we expect the shape to be approximately consistent with the possible VLTI detection of a very elongated or bi-lobated objects (see further below).

Considering the amount and the high quality of the tim-

ings for the stellar occultation of 2009 November 21, we chose to use the profile drawn by the chords as if it was obtained by disk-resolved imaging. This assumption was required to model the large concavity revealed by the interrupted chords at the South limb. We consider that this approach is fully justified and does not introduce a significant bias, since the number of positive chords available allowed a profile sampling with a resolution close to that obtained in disk-resolved imaging.

We thus ran KOALA to determine the best-fit period, spin, and 3-D shape to the lightcurves and stellar occultations, using the period and two spin locations determined above. We then checked the two solutions against the overall outline obtained from the MIDI-VLTI observations in 2005. The solution with a spin axis lying close to ECJ2000 (144° , -38°) provided a good match to the geometry derived from interferometric fitting (see Fig. 6 and Delbo et al. 2009). The resulting shape is shown in Fig. 5.

The resulting comparison has to be interpreted by taking into account the orientation of the VLTI baseline, essentially aligned along the direction of a protruding region in the NE direction. Clearly, this protrusion is the most relevant irregularity found by KOALA and can be related to the “secondary” body revealed by VLTI observations. It also happens to be well constrained by the occultation data. In fact, it appears close to the main concavity observed in November 2009 (and pointing downward in Fig. 2).

The 3-D model of Barbara derived here is made of 512 triangular facets³ and is scaled to absolute dimensions thanks to the contribution of stellar occultations. The mesh volume of our model is equivalent to a sphere having a diameter of 45.9 km.

These size measurements should be compared to the thermal diameter derived by AKARI (47.8 ± 0.68 km) and IRAS (43.7 ± 1 km). WISE derived 53.80 ± 1.12 km in the fully cryogenic phase (Masiero et al. 2011) and 45.29 ± 1.33 km during the 3-band cryogenic/post-cryogenic operation (Masiero et al. 2012). The first of the WISE measurements is clearly discrepant from all the other measurements. This discrepancy is due to the assumption made in Masiero et al.

³ The model is available on DAMIT

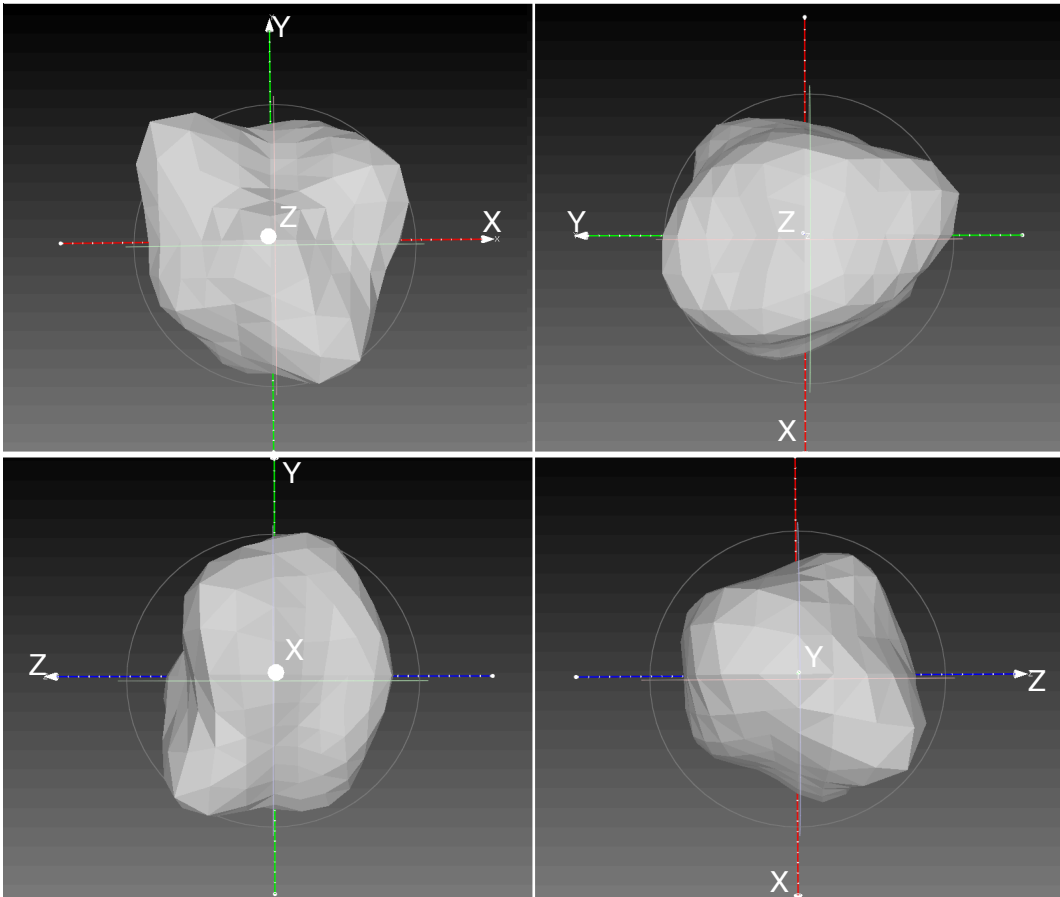


Figure 5. Four different projections of (234) Barbara. The two panels at the top have the South axis pointing upward. At bottom left, the South polar view is presented. At bottom right, a view at an intermediate aspect angle, strongly enhancing the visibility of concave areas. The z axis is parallel to the spin axis.

(2011) that the $4.6\text{-}\mu\text{m}$ albedos are equal to the $3.4\text{-}\mu\text{m}$ albedos, which biases the relative contributions of thermal flux and reflected sunlight in the WISE $4.6\text{-}\mu\text{m}$ data. By fitting the NEATM to the fully cryogenic, purely thermal WISE bands (12 and $22\text{ }\mu\text{m}$), we obtained a thermal diameter of $46 \pm 7\text{ km}$ (for details on our particular data selection criteria and procedure see ?, and references therein). Since the average of the four accepted values (45.7 km) is just 200 m less than our volume-equivalent diameter (0.4% relative difference), we consider that our model size is in excellent agreement with the thermal diameters.

Unfortunately, the sole published mass estimate (Fienga et al. 2010) is very poorly constrained ($0.44 \pm 1.45 \times 10^{18}\text{ kg}$) and cannot be used to derive the density or to draw any conclusion on the internal structure.

5 DISCUSSION

As suggested by stellar occultation and VLTI data, the shape of (234) Barbara is highly irregular with the presence of large concavities.

At all apparitions, the brightness variations seems to have approximately a similar amplitude, despite the change in aspect angle. This is probably to be ascribed to the ubiq-

uitous irregularities - present for all illumination and observation directions.

The derived shape, when rotated at an orientation corresponding to the VLTI observations, suggests an interpretation of the interferometric signal as the presence of a big prominence oriented along the baseline. Our results thus show that the VLTI observations can be explained without the presence of a large satellite. Stellar occultations also failed to show the presence of such a companion. Of course, this evidence cannot exclude that small satellites might be orbiting (234) Barbara (a few km in size), but they have no signatures in the available data.

Concerning the origin of the object and its collisional history, the absence of an identified family around (234) Barbara makes any interpretation loosely constrained.

A first possibility is that (234) Barbara is in fact the assemblage of two bodies of different sizes, resulting in a bilobated object. This interpretation could be consistent with the prominence revealed by VLTI. However, with the current limitations on the shape resolution and in absence of other constraints, this scenario remains rather speculative.

Another common factor of reshaping and excavation are, of course, non-disruptive impacts. In this case, we can reasonably assume that the convex hull of the shape of Barbara could represent the minimum volume that the original

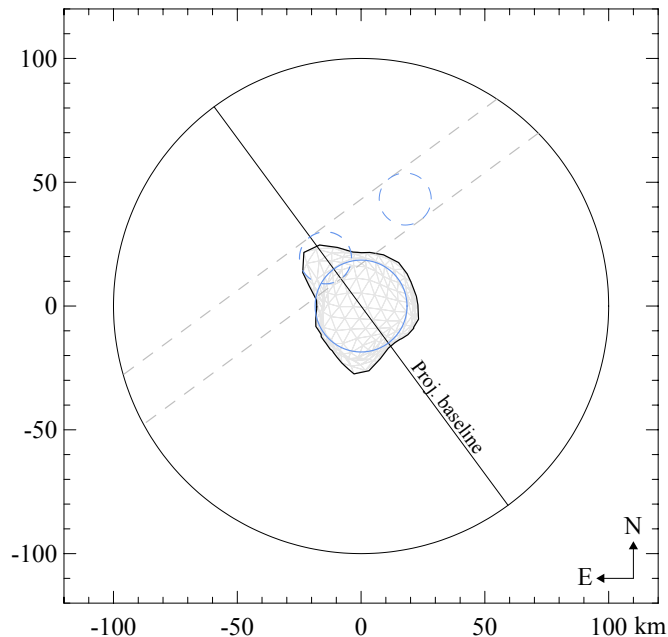


Figure 6. Comparison of the binary model of Barbara derived by Delbo et al. (2009) in blue lines with the KOALA shape model (black contour) at the time of VLTI observations. The irregular shape of Barbara mislead the interpretation, by mimicking the signal of a binary system projected on the VLTI baseline. As spatial resolution is missing in the direction perpendicular to the baseline, the dashed lines enclose possible locations for a satellite compatible with the VLTI signal.

body had, before being excavated by impacts. If no ejecta fall back is considered, we find an excavated volume 6.8% of the convex hull, representing $3.7 \times 10^{12} \text{ m}^3$. Since some fall-back probably occurred, the dislocation of the material could have been much more important.

According to Davis et al. (2002, Fig. 6), the probability that a 50-km object is a re-accumulated rubble-pile ranges from 45 to 70%.

The possibility of a rubble-pile structure is probably strengthened by the relatively slow rotation period of (234) Barbara. The role of non-destructive impacts on the evolution of rotation periods of relatively large asteroids has been the subject of several studies in the past. It has been suggested that collisions could diminish the angular momentum on average, carried away by escaping fragments, both in the case of craterization events (Dobrovolskis & Burns 1984, “angular momentum drain”) and in shattering impacts (Cellino et al. 1990, “angular momentum splash”). This last mechanism was invoked to explain the fact that asteroids smaller than ~ 100 km have shorter average rotation periods than larger ones (Farinella et al. 1992). More recently, detailed numerical simulations of impacts on rubble-pile asteroids (Takeda & Ohtsuki 2007b, 2009b) have shown that spin down is in fact a common consequence of impact events. If this was the case for (234) Barbara, we can suggest that one or more impacts subtracted angular momentum from an initially much larger body. Internal fragmentation during the process would then be a natural outcome of the collisional sequence that slowed down rotation and excavated the large concavities. A long history of collisional de-spinning and the ancient age of the material seem to suggest a self-consistent

scenario, supporting the idea that Barbarians might be very old objects.

The data that we have at our disposal do not show the evidence of a Barbara family, suggesting that the impact events could be very old, and the hypothetical family is now indistinguishable from the background. Future spectroscopic surveys could permit the detection of an anomalous concentrations of L/Ld-type asteroids in the corresponding region of the orbital elements space.

6 CONCLUSIONS

Stellar occultations, coupled to photometry, are a powerful tool to characterize bodies that present concave features. They were seminal in obtaining the shape of (234) Barbara, appearing to be very irregular and dominated by large concavities. One of these concavities is particularly extended and well sampled by our occultations.

The non-convex model that we present can still be improved and confirmed by more extensive observing campaigns, however it appears to explain the observations previously obtained at VLTI. The sky projection of the largest prominence present on the object is aligned to the VLTI baseline at the epoch of observation, mimicking the signature of a bi-lobated object.

Even if apparently our results seem to support the direct relation of concavities to polarization properties (Cellino et al. 2006), this is valid only in the empirical sense, as it has no theoretical ground at present. In principle it might be possible that the presence of concavities is related to polarimetry only in an indirect sense. For example, the collisional excavation could have changed the composition or the texture of the surface, by exposing layers that remain otherwise hidden, or by redistributing/ejecting a layer of surface regolith. On the other hand, as the “barbarians” share common spectral properties, we cannot exclude that their peculiar polarimetry is essentially due to their bulk composition. The recent discovery of several Barbarians inside the Watsonia family seems to corroborate this hypothesis, as it implies the transmission by direct heritage of the Barbarian properties from the parent body to family members (Cellino et al. 2014).

We underline the role played in this work by a large collaboration of amateur and professional astronomers, both in obtaining an adequate photometric coverage and in securing the positive results of the two occultations that have allowed us to constrain the concavities. The long rotation period, and its commensurability to the duration of Earth’s day is an obstacle to an efficient coverage of the object rotation.

A network of observers at different longitudes constitute a clear advantage that we will try to exploit in future photometric campaigns devoted to barbarian asteroids. Obtaining more shapes of the Barbarians, polarimetric measurements and near-infrared spectra to confirm the presence of spinel-rich inclusions is required to better understand such objects that could represent a rare sample of CAI-rich Solar System bodies, dating back to the first phases of Solar System formation.

ACKNOWLEDGMENTS

This research used the *Miriade* VO tool developed at IM-CCE (Berthier et al. 2008) and MP3C at OCA (Delbo' and Tanga, <http://mp3c.oca.eu/>). We acknowledge the financial support of the occultation activity carried on by OCA members, from the BQR program of the Observatoire de la Côte d'Azur, the Action Spécifique Gaia, and the Programme Nationale de Planétologie. The work of JH was carried under the contract 11-BS56-008 (SHOCKS) of the French Agence Nationale de la Recherche (ANR). We thank the developers and maintainers of Meshlab and VO Topcat software. TRAPPIST is a project funded by the Belgian Fund for Scientific Research (Fonds de la Recherche Scientifique, F.R.S FNRS) under grant FRFC 2.5.594.09.F, with the participation of the Swiss National Science Foundation (SNF). E. Jehin and M. Gillon are FNRS Research Associates, J. Manfroid is Research Director FNRS. A. Matter acknowledges financial support from the Centre National d'Etudes Spatiales (CNES). We thank all the members of "Agrupación Astronómica de Fuerteventura" for the coordination of the observations and the "Cabildo de Fuerteventura" for the logistic support in Tefía observatory. Also, S. Degenhart is acknowledged for the organization of the campaign in the U.S.A. that yielded the second occultation profile presented in this paper.

REFERENCES

Belskaya I. N., Fornasier S., Krugly Y. N., Shevchenko V. G., Gaftonyuk N. M., Barucci M. A., Fulchignoni M., Gil-Hutton R. G., 2010, *Astronomy and Astrophysics*, 515, A29
 Berthier J., Hestroffer D., Carry B., Āurech J., Tanga P., Delbo M., Vachier F., 2008, *LPI Contributions*, 1405, 8374
 Bottke W. F., Vokrouhlick D., Rubincam D. P., Nesvorn D., 2006, *Annual Review of Earth and Planetary Sciences*, 34, 157
 Burbine T. H., Gaffey M. J., Bell J. F., 1992, *Meteoritics*, 27, 424
 Bus S. J., Binzel R. P., 2002, *Icarus*, 158, 146
 Carry B., Dumas C., Kaasalainen M., Berthier J., Merline W. J., Erard S., Conrad A. R., Drummond J. D., Hestroffer D., Fulchignoni M., Fusco T., 2010, *Icarus*, 205, 460
 Carry B., Kaasalainen M., Merline W. J., Müller T. G., Jorda L., Drummond J. D., Berthier J., O'Rourke L., Āurech J., Küppers M., Conrad A. R., Dumas C., Sierks H., the OSIRIS Team 2012, *Planetary and Space Science*, in press
 Cellino A., Bagnulo S., Tanga P., Novaković B., Delbò M., 2014, *MNRAS*
 Cellino A., Belskaya I., Bendjoya P., Martino M. D., Gil-Hutton R., Muinonen K., Tedesco E., 2006, *Icarus*, 180, 565
 Cellino A., Zappalá V., Davis D., Farinella P., Paolicchi P., 1990, *Icarus*, 87, 391
 Davis D. R., Durda D. D., Marzari F., Campo Bagatin A., Gil-Hutton R., 2002, *Asteroids III*, pp 545–558
 Delbo M., Ligorì S., Matter A., Cellino A., Berthier J., 2009, *Astrophysical Journal*, 694, 1228

Dobrovolskis A. R., Burns J. A., 1984, *Icarus*, 57, 464
 Dunham D. W., Herald D., Frappa E., Hayamizu T., Talbot J., Timerson B., 2011, *Asteroid Occultations*, NASA Planetary Data System
 Āurech J., Sidorin V., Kaasalainen M., 2010, *Astronomy and Astrophysics*, 513, A46
 Farinella P., Davis D., Paolicchi P., Cellino A., Zappalá V., 1992, *Astron. A.*, 253, 604
 Fienga A., Manche H., Kuchynka P., Laskar J., Gastineau M., 2010, *Scientific Notes*
 Gil-Hutton R., Mesa V., Cellino A., Bendjoya P., Pealoza L., Lovos F., 2008, *Astronomy and Astrophysics*, 482, 309
 Hanuš J., Āurech J., Brož M., Marciniak A., Warner B. D., Pilcher F., Stephens R., Behrend R., Carry B., Āapek D., Antonini P., Waelchli N., Wagrez K., Wücher H., 2013, *Astron. A.*, 551, A67
 Holsapple K. A., 2007, *Icarus*, 187, 500
 Holsapple K. A., Housen K. R., 2012, *Icarus*, 221, 875
 Johansen A., Lacerda P., 2010, *MNRAS*, 404, 475
 Kaasalainen M., 2011, *Inverse Problems and Imaging*, 5, 37
 Kaasalainen M., Torppa J., 2001, *Icarus*, 153, 24
 Kaasalainen M., Torppa J., Muinonen K., 2001, *Icarus*, 153, 37
 Leinert C., Graser U., Przygodda F., Waters L. B. F. M., Perrin G., Jaffe W., Lopez B., Bakker E. J., Böhm A., von der Lühe O., Wagner K., 2003, *Astrophysics and Space Science*, 286, 73
 Marzari F., Rossi A., Scheeres D. J., 2011, *Icarus*, 214, 622
 Masiero J., Cellino A., 2009, *Icarus*, 199, 333
 Masiero J. R., Mainzer A. K., Grav T., Bauer J. M., Cutri R. M., Dailey J., Eisenhardt P. R. M., McMillan R. S., Spahr T. B., Skrutskie M. F., Tholen D., Walker R. G., Wright E. L., DeBaun E., Elsbury D., Gautier IV T., Gomillion S., Wilkins A., 2011, *Astron. J.*, 741, 68
 Masiero J. R., Mainzer A. K., Grav T., Bauer J. M., Cutri R. M., Nugent C., Cabrera M. S., 2012, *Astron. J.*, 759, L8
 Muñoz O., Volten H., Vermeulen K., de Haan J. F., Vassen W., Hovenier J. W., 2000, *Scattering Matrices of Fly-ash and Green Clay Particles*. pp 45–48
 Muinonen K., Lumme K., Peltoniemi J., Irvine W. M., 1989, *Applied Optics*, 28, 3051
 Schober H. J., 1981, *Astronomy and Astrophysics*, 96, 302
 Shkuratov Y., Ovcharenko A., Zubko E., Miloslavskaya O., Muinonen K., Piironen J., Nelson R., Smythe W., Rosenbush V., Helfenstein P., 2002, *Icarus*, 159, 396
 Shkuratov Y. G., Muinonen K., Bowell E., Lumme K., Peltoniemi J. I., Kreslavsky M. A., Stankevich D. G., Tishkovetz V. P., Opanasenko N. V., Melkumova L. Y., 1994, *Earth Moon and Planets*, 65, 201
 Sunshine J. M., Connolly H. C., McCoy T. J., Bus S. J., La Croix L. M., 2008, *Science*, 320, 514
 Takeda T., Ohtsuki K., 2007a, *Icarus*, 189, 256
 Takeda T., Ohtsuki K., 2007b, *Icarus*, 189, 256
 Takeda T., Ohtsuki K., 2009a, *Icarus*, 202, 514
 Takeda T., Ohtsuki K., 2009b, *Icarus*, 202, 514
 Tedesco E. F., Noah P. V., Noah M. C., Price S. D., 2002, *Astronomical Journal*, 123, 1056
 Zellner B., Leake M., Lebertre T., Duseaux M., Dollfus A., 1977, in Merrill R. B., ed., *Lunar and Planetary Science Conference Proceedings Vol. 8 of Lunar and Plane-*

tary Science Conference Proceedings, The asteroid albedo scale. I - Laboratory polarimetry of meteorites. pp 1091–1110